R. & M. No. 3105
(19,306)
A.R.C. Technical Report

MINISTRY OF SUPPLY

AERONAUTICAL RESEARCH COUNCIL
REPORTS AND MEMORANDA

Aerodynamic Characteristics in the Approach, Superfine and Negative Pitch Ranges of Two Four-Bladed Propellers with N.A.C.A. Series 16 Blade Sections.

A report of Tests carried out Jointly by the Technical Staffs of de Havilland Propellers, Limited, and Rotol, Limited.

LONDON : HER MAJESTY'S STATIONERY OFFICE
1959
PRICE 8*s*. 6*d*. NET

Aerodynamic Characteristics in the Approach, Superfine and Negative Pitch Ranges of Two Four-Bladed Propellers with N.A.C.A. Series 16 Blade Sections.

A Report of Tests carried out Jointly by the Technical Staffs of de Havilland Propellers, Limited, and Rotol, Limited.

Reports and Memoranda No. 3105*

April, 1957

Summary.—Tests were conducted on two similar full-scale propellers in the 24-ft Wind Tunnel at the Royal Aircraft Establishment by representatives of Rotol, Ltd. and de Havilland Propellers, Ltd. to measure the aerodynamic characteristics over a blade-angle range of − 20 deg to + 40 deg, measured at the 0·7 radius, and over a range of advance ratio of 0·1 to 2·4.

---

1. *Reason for Test.*—The design of propellers for turbine engines has involved consideration of propeller operating conditions which were not of great significance in the case of piston-engined applications, and for which there existed very little basic test data. It has been found necessary to give particular consideration to the behaviour of the aircraft, engine and propeller when the latter is operating in the blade-angle ranges which occur during landing approach, ground manoeuvring and negative-thrust braked landings. There existed an urgent need for experimental data on the characteristics of propellers having plan-forms representative of present-day designs, and incorporating NACA Series 16 sections, under the above operating conditions.

A test programme to supply sufficient data to cover the immediate needs of the propeller industry was drawn up, and the purpose of this report is to present the results which were obtained from the tests.

2. *Introduction.*—The aerodynamic characteristics of two 10-ft diameter four-blade propellers were investigated. The blades were of identical plan-form, twist and thickness/chord and differed only in respect of integrated-design lift coefficient.

Blade design RA25842 had an integrated design lift coefficient of 0·55 and blade design RA25872 an integrated design lift coefficient of 0·25.

The propellers were tested at forward speeds up to normal approach speed over the following range of blade angles (measured at the 0·7 radius):

High cambered blade, design RA25842	− 20 to + 25 deg
Low cambered blade, design RA25872	− 20 to + 40 deg.

Values of power absorption, thrust and blade twisting moments were recorded.

---

* Report received 31st May, 1957.

3. *Description of Test Equipment.*—3.1. *Electric Motor.*—A 1,500 b.h.p. squirrel-cage variable-frequency induction motor, enclosed in a nacelle supported by struts (*see* Fig. 14), was used to provide or absorb propeller power. The input power to the motor was measured and hence, by making allowance for losses, the power absorbed by the propeller was calculated.

3.2. *Tunnel and Balance.*—The normal tunnel balance was used to measure the propeller thrust and drag. A full description of the balance and tunnel may be found in Ref. 1.

3.3. *Propeller.*—Each propeller had four blades with NACA Series 16 sections; the blade characteristics are shown in Fig. 1. One set of blades was of the design used in the standard *Viscount* propeller (Rotol blade design RA25842) and the blades each had an integrated design lift coefficient of 0·55. The other set of blades to design RA25872 had an integrated design lift coefficient of 0·25, the distribution being exactly as design RA25842. The activity factor of each blade was 142.

The normal constant-speeding pitch-change mechanism was removed and the blade angle locked at the desired value by means of the standard R.A.E. pitch-locking system. The blade angle could be adjusted manually when the propeller was stationary and was measured at the master station (0·7 radius) by means of a clinometer.

3.4. *Spinner.*—During the main tests a *Viscount*-type spinner was fitted to the propellers. It was necessary to cut a hole of about $1\frac{1}{2}$ in. diameter in the nose to lead out the support and wires from the mercury slip rings.

3.5. *Strain-Gauge Equipment.*—The equipment used to measure the twisting moment on the blade consisted of thrust rings inserted in the links between the root of the blade and the pitch-locking mechanism, the strain-gauges being cemented to the rings. Fig. 15 shows the lay-out of the apparatus. It is necessary for small changes in blade angle to occur but the thrust rings were designed to limit the pitch movement to about ten minutes of arc. The strain-gauges were connected as a full bridge with external balance and slide wire, the bridge being polarised by a 200-c.p.s., 35-volt supply. The rings were calibrated on a Denison tensile testing machine, load applied (lb) being plotted against slide-wire dial reading.

The leads from the strain-gauges were taken to a set of mercury slip rings, the fixed parts of which were prevented from rotating by means of a fixed rod leading out of a hole in the nose of the spinner and supported by four wires across the mouth of the tunnel, the leads from the slip rings being taped to one of the support wires. The mercury slip rings were not in circuit when the strain-gauge calibration was performed but other tests had ensured that at all speeds the contact resistance was negligible.

Thrust rings were placed in the links to all four blades but measurements were taken from the strain gauges on one ring only.

3.6. *Pitot Rake.*—The rake consisted of seven pitot-tubes placed with their open ends 14 in. behind the blade centre-line and aligned parallel to the propeller axis. The tubes were placed at the following distances from the motor centre-line:

2·25, 2·75, 3·25, 3·75, 4·25, 4·63 and 4·87 ft,

i.e., at 0·45, 0·55, 0·65, 0·75, 0·85, 0·925 and 0·975 of the propeller tip radius.

The diameter of the motor nacelle in line with the open ends of the tubes was 0·35 of that of the propeller. The pitot-tubes were connected to a multi-bank manometer in the balance house where the pressures were recorded by an observer.

4. *Test Procedure.*—4.1. *Preliminary Tests.*—In order to obtain the value of drag for the nacelle and supporting structure, a spinner without a propeller was fitted to the body and drag values were obtained at intervals throughout the speed range of the tunnel. Unfortunately, it was not possible to use the same spinner as for the rest of the tests, the spinner for the preliminary tests being larger and fitting the motor housing better. Previous experience of testing propellers in this tunnel on the same nacelle arrangement had shown that variations of body drag due to small changes in spinner diameter were negligible.

To check that the effect of the strain-gauge equipment, *i.e.*, the hole in the spinner, support rod and wire, and presence of electrical leads in front of the propeller, was negligible, a run at a blade angle of 15 deg as completed with the strain-gauge apparatus in position. The equipment was then removed, the hole in the spinner sealed and the run repeated. The run was repeated a third time with the strain-gauge apparatus in position again. It was found that within the limits of experimental accuracy the presence of this equipment did not affect the results obtained.

4.2. *Major Tests.*—Tests of the propellers were carried out at blade angles from − 20 to + 25 deg for the high camber blade and from − 20 to + 40 deg for the low camber blade, the blade angle being varied in 5 deg increments. The time factor prevented the propeller characteristics for blade angles between + 25 and + 40 deg being investigated on both propellers since it was necessary to strip and re-index them in order to cover this angle range. Tests were run at constant rotational speed, the range of advance ratio being obtained by varying the tunnel air speed. Values of propeller thrust or drag, power required or absorbed and forces in link were noted.

4.3. *Wake Survey.*—After these tests were finished a wake survey was carried out with the pitot rake using the propeller with high cambered blades (design RA25842). Runs were carried out for a range of tunnel speeds and propeller r.p.m.

5. *Results and Discussion.*—5.1. *Power Absorption and Thrust Measurements.*—The results obtained are shown in the form of graphs of power coefficient (C_P) against advance ratio (J) at constant blade angles ($\theta_{.7}$) and thrust coefficient (C_T) against advance ratio at the same blade angles. The accuracy that could be obtained depended on the propeller blade angle. At positive angles the thrust could be measured to within ± 15 lb. At some negative blade angles and high forward speeds, propeller flutter and severe turbulence in the working-section of the tunnel were encountered; under these conditions the balance could only be read to within about ± 50 lb.

Propeller r.p.m. were set to within ± 1 r.p.m., except for the runs at angles of $\theta_{.7} = + 30$, + 35, + 40 deg on the propeller with low cambered blades, when a breakdown in a tachogenerator put the normal r.p.m. measuring equipment out of action. Propeller r.p.m. readings were then taken on another instrument, which could not be read better than about ± 10 r.p.m. There is much more scatter in the results presented for these blade angles and it is believed to be due partly to inaccuracy in the recorded value of propeller r.p.m. It will be noted on plotting the results presented in Tables 1 and 2 that, at a given value of blade angle and advance ratio, there does appear to be a variation of thrust and power coefficient with propeller r.p.m., which suggests that there is a Mach-number or Reynolds-number effect present.

Examination of Figs. 2 to 7 inclusive shows that for a given value of blade angle and advance ratio, the propeller with high camber blades has a more positive power and thrust coefficient than the one with low camber blades.

5.2. Wake Survey.—The local thrust grading is given by (Ref. 2)

$$\frac{dT}{dr} = 2\pi r(H_r - H_0) ,$$

where H_r is the total head immediately behind the propeller disc at radius r and H_0 is the total head upstream of the disc.

The total head H_0 was obtained from a pressure measurement upstream of the propeller, and values of H_r were obtained from readings of the manometer attached to the pitot rake.

The results of the wake survey are presented in tabular form (Table 3) as the elemental thrust coefficient dC_T/dx at the blade stations at which the pitots were placed. The results are also shown in graphical form in Figs. 8 to 13.

It was found that owing to the contraction of the slipstream behind the propeller, the pitot tubes, corresponding to the blade stations $x = 0 \cdot 925$ and $0 \cdot 975$, were often in the tip vortices and the manometer readings obtained fluctuated greatly. The limits of these oscillations were recorded and are shown in the results.

5.3. *Aerodynamic Twisting Moments.*—When provisioning for these measurements to be taken it had been anticipated that the friction in the blade retention of the propeller used for these tests would be negligible when the propeller was rotating. With this proviso the derivation of aerodynamic twisting moments from the measured values would have been straightforward.

The results obtained suggested that there was in fact some friction present while the propeller was rotating, and that this friction was variable and was a function of the time of running at a given blade angle. In an attempt to make appropriate allowances for this friction in the analysis of the strain-gauge observations, readings were taken of the pressures in the pitch-change oil lines of a propeller installed and running on an engine to obtain an estimate of the friction present.

However, examination of the results indicated that these measurements of friction existing in a normal ' constant-speeding ' propeller were not an adequate measure of that existing when the propeller blades were mechanically locked, as in the wind-tunnel tests. It was therefore concluded that the degree of variation of the friction was of sufficient magnitude in comparison with the anticipated value of aerodynamic twisting moment that no reliable results could be obtained from the investigation.

6. *Conclusion.*—Tests have been carried out in the R.A.E. 24-ft Wind Tunnel to investigate the aerodynamic characteristics of two *Viscount*-type propellers over the range of blade angles, propeller r.p.m. and forward speed likely to be encountered during aircraft landing approach, ground manoeuvring and negative thrust braked landings. The results of these tests will enable performance estimates to be made for the range of operating conditions covered with reliability greater than could hitherto be achieved.

Ultimately, it will be necessary to correlate these results with previously existing data to establish factors to correct for variations in blade plan-form and camber. In the meantime the results may be used to obtain estimates for propellers with NACA Series 16 section blades of similar shape, by ratioing the values of C_P and C_T directly as ' total activity factor '. Allowance should be made in the blade angle for the difference between the ' no-lift angle ' of the section at $0 \cdot 7$ radius of the test blade and the blade under consideration.

LIST OF SYMBOLS

c	Blade chord (ft)
C_{LD}	Blade-section-design lift coefficient
C_P	Power coefficient
	$= \dfrac{P}{\rho n^3 D^5}$
C_T	Thrust coefficient
	$= \dfrac{T}{\rho n^2 D^4}$
D	Propeller diameter (ft)
F	Force measured by strain-gauge
J	Propeller advance ratio
	$= \dfrac{v}{nD}$
H_0	Total head upstream of propeller disc
H_r	Total head immediately behind the propeller disc at radius r
n	Propeller rotational speed (r.p.s.)
P	Power absorbed by propeller (ft lb/sec)
Q	Total torque on blade tending to decrease pitch
r	Radius to blade element
R	Propeller tip radius (ft)
t	Blade-section maximum thickness (ft)
T	Propeller thrust (lb)
v	Air speed (tunnel speed) (ft/sec)
θ	Blade angle (deg)
$\theta_{.7}$	Blade angle at 0·7 tip radius (deg)
γ, δ	*See* Fig. 8.
ρ	Mass density of air slugs/ft^3

REFERENCES

No.	*Author*	*Title, etc.*
1	W. G. Jennings, A. Terry and P. J. Pearsall	Preliminary calibration of the 24-ft Wind Tunnel, R.A.E., with a short description of the tunnel. R. & M. 1720. 1936.
2	R. C. Pankhurst and D. W. Holder	*Wind-Tunnel Technique.* Pitman & Sons, Ltd. 1952.

TABLE 1

Results Obtained from Major Tests

Blade Design RA25842

$\theta_{.7} = 24° 40'$				$\theta_{.7} = 20°$			
N	J	C_P	C_T	N	J	C_P	C_T
400	0·465	+0·164	+0·198	400	0·466	+0·102	+0·139
400	1·050	+0·058	+0·043	400	1·360	−0·121	−0·193
400	1·357	−0·054	−0·082	400	1·815	−0·315	−0·431
400	1·810	−0·282	−0·312	400	2·120	−0·414	−0·552
400	2·115	−0·418	−0·445	400	2·420	−0·506	−0·675
400	2·415	−0·530	−0·560	700	0·267	+0·121	+0·184
700	0·345	+0·184	+0·222	700	0·779	+0·060	+0·054
700	0·775	0·127	0·126	700	1·210	−0·059	−0·127
700	1·034	+0·062	+0·042	700	1·382	−0·133	−0·214
700	1·382	−0·070	−0·100	1000	0·300	+0·125	+0·184
1000	0·299	+0·198	+0·233	1000	0·545	0·101	+0·123
1000	0·545	0·169	0·188	1000	0·966		−0·021
1000	0·968	0·082	0·063	1300	0·274	0·133	+0·191
1300	0·272	0·207	0·240	1300	0·420	0·117	0·157
1300	0·418	0·190	0·217	1300	0·743	0·064	0·058
1300	0·745	0·134	0·128	1600	0·264	0·142	0·200
1500	0·282	0·214	0·252	1600	0·341	0·131	0·180
1500	0·363	0·201	0·230	1600	0·606	+0·091	+0·101
1500	0·484	0·184	0·205				
1500	0·645	+0·152	+0·156				
190	1·280	0	−0·038	230	1·082	0	−0·050
385	1·250	0	−0·031	463	1·045	0	−0·037
587	1·235	0	−0·030	710	1·020	0	−0·037
785	1·230	0	−0·031	960	1·000	0	−0·038
$\theta_{.7} = 15°$				$\theta_{.7} = 10°$			
400	0·470	+0·061	+0·085	400	0·460	+0·033	+0·028
400	1·368	−0·150	−0·309	400	1·345	−0·132	−0·400
400	1·820	−0·296	−0·533	400	1·795	−0·233	−0·608
400	2·130	−0·375	−0·660	400	2·090	−0·292	−0·732
400	2·430	−0·453	−0·787	400	2·400	−0·346	−0·874
700	0·268	+0·073	+0·129	700	0·263	+0·042	+0·076
700	0·782	+0·011	−0·027	700	0·769	−0·005	−0·111
700	1·215	−0·100	−0·240	700	1·025	−0·045	−0·236
700	1·390	−0·153	−0·329	700	1·370	−0·128	−0·407
1000	0·243	+0·076	+0·136	1000	0·184	+0·046	+0·091
1000	0·548	+0·050	+0·055	1000	0·540	+0·025	−0·010
1000	0·850	−0·008	−0·068	1000	0·960	−0·035	−0·204
1000	0·972	−0·037	−0·129	1300	0·184	+0·048	+0·098
1300	0·232	+0·078	+0·135	1300	0·414	+0·035	+0·028
1300	0·422	0·064	+0·090	1300	0·739	−0·001	−0·112
1300	0·747	0·013	−0·029	1600	0·185	+0·048	+0·093
1600	0·228	0·082	+0·142	1600	0·338	0·042	+0·052
1600	0·343	0·074	0·114	1600	0·600	+0·018	−0·049
1600	0·610	+0·038	+0·021				
283	0·855	0	−0·054	300	0·796	0	−0·100
570	0·854	0	−0·057	630	0·760	0	−0·098
875	0·833	0	−0·056	970	0·740	0	−0·099
1185	0·820	0	−0·059	1290	0·743	0	−0·107

TABLE 1—*continued*

$\theta_{\cdot 7} = +5°$				$\theta_{\cdot 7} = 0°$			
N	J	C_P	C_T	N	J	C_P	C_T
400	1·355	−0·079	−0·486	400	0·462	+0·033	−0·064
400	1·808	−0·142	−0·690	400	1·350	+0·004	−0·554
400	2·105	−0·181	−0·837	400	1·800	−0·025	−0·765
400	2·400	−0·218	−0·969	400	2·100	−0·044	−0·900
700	0·266	+0·029	+0·023	400	2·395	−0·060	−1·041
700	0·775	+0·009	−0·178	700	0·264	+0·027	−0·009
700	1·202	−0·048	−0·414	700	0·772	0·046	−0·228
700	1·282	−0·060	−0·457	700	1·200	0·024	−0·472
1000	0·542	+0·023	−0·069	700	1·286	0·016	−0·518
1000	0·844	+0·003	−0·220	1000	0·185	0·024	+0·005
1000	0·900	−0·002	−0·255	1000	0·540	0·040	−0·107
1300	0·143	+0·029	+0·045	1000	0·840	0·050	−0·274
1300	0·418	0·027	−0·026	1000	0·900	0·048	−0·308
1300	0·690	0·017	−0·150	1300	0·143	0·024	+0·009
1600	0·116	0·030	+0·028	1300	0·416	0·035	−0·039
1600	0·340	0·030	−0·003	1300	0·555	0·043	−0·118
1600	0·523	+0·026	−0·077	1300	0·648	0·047	−0·165
				1600	0·116	0·024	+0·013
263	0·914	0	−0·232	1600	0·338	+0·033	−0·037
540	0·890	0	−0·239				
810	0·910	0	−0·244	240	1·500	0	−0·642
1000	0·902	0	−0·249	328	1·460	0	−0·616
				413	1·450	0	−0·608
				495	1·455	0	−0·607
				573	1·470	0	−0·610
				647	1·480	0	−0·615

$\theta_{\cdot 7} = -5°$				$\theta_{\cdot 7} = -10°$			
400	1·352	0·107	−0·600	400	1·346	0·230	−0·640
400	1·800	0·105	−0·825	400	1·790	0·262	−0·874
400	2·100	0·105	−0·975	400	2·100	0·293	−1·023
400	2·400	0·108	−1·110	400	2·400	0·313	−1·150
700	0·265	0·041	−0·042	700	0·264	0·078	−0·068
700	0·774	0·093	−0·260	700	0·772	0·146	−0·276
700	1·034	0·114	−0·431	700	1·030	0·206	−0·449
700	1·290	0·113	−0·569	700	1·290	0·233	−0·597
1000	0·542	0·064	−0·132	1000	0·540	0·107	−0·160
1000	0·723	0·093	−0·231	1000	0·720	0·138	−0·244
1000	0·844	0·104	−0·307	1000	0·840	0·163	−0·316
1300	0·143	0·034	−0·019	1300	0·143	0·081	−0·059
1300	0·417	0·051	−0·084	1300	0·416	0·090	−0·125
1300	0·556	0·066	−0·142	1300	0·600	0·116	−0·186
1600	0·115	0·035	−0·014	1600	0·116	0·080	−0·055
				1600	0·220	0·073	

TABLE 1—*continued*

$\theta_{.7} = -15°$				$\theta_{.7} = -20°$			
N	J	C_P	C_T	N	J	C_P	C_T
400	1·355	0·365	−0·665	400	0·462	0·237	−0·211
400	1·800	0·426	−0·920	400	1·350	0·524	−0·690
400	2·100	0·461	−1·036	400	1·800	0·613	−0·947
400	2·400	0·509	−1·155	400	2·100	0·662	−1·060
700	0·265	0·140	−0·100	400	2·400	0·728	−1·170
700	0·775	0·202	−0·290	700	0·265	0·214	
700	1·030	0·298	−0·467	700	0·773	0·288	−0·327
700	1·290	0·362	−0·626	700	1·030	0·386	−0·476
1000	0·185	0·138	−0·100	700	1·290	0·507	−0·650
1000	0·543	0·168	−0·212	1000	0·185	0·197	−0·130
1000	0·843	0·225	−0·330	1000	0·542	0·244	−0·237
1300	0·143	0·138	−0·097	1000	0·843	0·285	−0·352
1300	0·418	0·150	−0·166	1300	0·143	0·193	−0·123
				1300	0·271	0·206	−0·164

TABLE 2

Results Obtained from Major Tests

Blade Design RA25872

$\theta_{\cdot 7} = 40^\circ$				$\theta_{\cdot 7} = 35^\circ$			
N	J	C_P	C_T	N	J	C_P	C_T
430	0·555	+0·500	+0·280	430	0·555	+0·375	+0·247
430	1·250	0·302	0·183	430	1·250	0·147	+0·101
430	1·810	+0·070	+0·028	430	1·670	+0·034	−0·034
430	2·370	−0·294	−0·151	430	2·370	−0·476	−0·306
730	0·411	+0·505	+0·283	730	0·410	+0·386	+0·266
730	0·740	0·453	0·255	730	0·736	0·302	0·213
730	1·070	0·350	0·205	730	1·065	0·211	0·150
730	1·400	0·238	0·140	730	1·390	0·097	0·061
1030	0·525	0·526	0·282	1200	0·450	0·446	0·281
1030	0·760	0·487	0·261	1200	0·650	0·402	0·251
1030	0·990	+0·406	+0·226	1200	0·900	+0·320	+0·210

$\theta_{\cdot 7} = 30^\circ$				$\theta_{\cdot 7} = 25^\circ$			
430	1·250	+0·020	+0·015	400	0·466	+0·155	+0·178
430	1·670	−0·184	−0·157	400	1·358	−0·100	−0·099
430	2·230	−0·462	−0·393	400	2·420	−0·584	−0·555
730	0·736	+0·177	+0·165	700	0·344	−0·178	+0·195
730	0·980	0·121	+0·098	700	0·775	+0·100	+0·102
730	1·310	0·008	0	700	1·380	−0·106	−0·112
1320	0·410	0·302	+0·242	1000	0·299	+0·193	+0·207
1320	0·544	0·270	0·220	1000	0·543	0·150	0·164
1320	0·725	+0·194	+0·184	1000	0·967	0·053	0·041
				1000	0·724	0·113	0·114
				1300	0·279	0·202	0·212
				1300	0·419	0·176	0·189
				1300	0·745	0·109	0·107
				1500	0·281	0·207	0·211
				1500	0·362	0·190	0·198
				1500	0·645	+0·131	+0·138
				202	1·190	0	−0·022
				421	1·150	0	−0·010
				634	1·140	0	−0·014
				850	1·130	0	−0·014

TABLE 2—*continued*

$\theta_{.7} = 20°$				$\theta_{.7} = 15°$			
N	J	C_P	C_T	N	J	C_P	C_T
400	0·476	+0·083	+0·127	400	0·463		+0·061
400	1·345	—0·160	—0·195	400	1·348	—0·183	—0·308
400	2·395	—0·564	—0·664	400	2·400	—0·488	—0·796
700	0·263	+0·135	+0·171	700	0·265	+0·059	+0·108
700	0·769	+0·043	+0·045	700	0·773	—0·012	—0·043
700	1·365	—0·163	—0·212	700	1·370	—0·183	+0·336
1000	0·240	+0·127	+0·177	1000	0·240	+0·063	0·113
1000	0·539	0·090	0·114	1000	0·541	+0·031	+0·036
1000	0·717	+0·057	+0·060	1000	0·960	—0·062	—0·136
1000	0·956	—0·006	—0·022	1300	0·228	+0·064	+0·117
1300	0·276	+0·125	+0·173	1300	0·416	+0·048	+0·072
1300	0·414	0·107	0·146	1300	0·740	—0·008	—0·040
1300	0·736	0·049	0·051	1600	0·225	+0·068	+0·122
1600	0·262	0·138	0·183	1600	0·339	0·057	0·093
1600	0·338	0·125	0·164	1600	0·601	+0·018	+0·007
1600	0·600	+0·080	+0·093				
238	1·000	0	—0·019	310	0·772	0	
505	0·946	0	—0·016	478	0·751	0	
762	0·940	0	—0·018	650	0·736	0	
1017	0·938	0	—0·019	820	0·730	0	—0·029
				996	0·722	0	—0·029
				1170	0·715	0	—0·029
				1350	0·710	0	—0·031

$\theta_{.7} = 10°$				$\theta_{.7} = 5°$			
400	0·462	+0·016	+0·001	400	0·464	+0·010	—0·036
400	1·349	—0·159	—0·417	400	1·346	—0·103	—0·495
400	2·400	—0·386	—0·900	400	2·400	—0·255	—0·992
700	0·265	+0·029	—0·055	700	0·265	+0·016	+0·014
700	0·773	—0·030	—0·122	700	0·770	—0·016	—0·187
700	1·370	—0·157	—0·424	700	1·285	—0·087	—0·462
1000	0·185	+0·035	+0·072	1000	0·186	+0·018	+0·033
1000	0·540	+0·006	—0·027	1000	0·540	+0·005	—0·077
1000	0·960	—0·063	—0·224	1000	0·900	—0·027	—0·259
1300	0·185	+0·035	+0·073	1300	0·143	+0·019	+0·037
1300	0·416	+0·019	+0·013	1300	0·416	+0·011	—0·033
1300	0·739	—0·023	—0·117	1300	0·691	—0·006	—0·154
1600	0·186	+0·035	+0·075	1600	0·150	+0·020	+0·036
1600	0·338	+0·026	+0·036	1600	0·338	0·015	—0·012
1600	0·601	—0·003	—0·060	1600	0·562	+0·004	—0·093
380	0·631	0	—0·054	370	0·650	0	—0·119
787	0·610	0	—0·050	565	0·636	0	—0·116
1212	0·591	0	—0·050	767	0·626	0	—0·114
1628	0·589	0	—0·055	963	0·624	0	—0·113
				1155	0·623	0	—0·117
				1330	0·650	0	—0·123
				1415	0·635	0	—0·127

TABLE 2—*continued*

$\theta_{\cdot 7} = 0°$

N	J	C_P	C_T
400	0·461	+0·020	—0·062
400	1·349	—0·023	—0·570
400	2·395	—0·101	—1·070
700	0·264	+0·016	—0·013
700	0·760	+0·018	—0·224
700	1·285	—0·013	—0·529
1000	0·185	+0·014	—0·001
1000	0·540	0·019	—0·106
1000	0·900	0·022	—0·312
1300	0·142	0·014	+0·006
1300	0·415	0·018	—0·060
1300	0·692	0·025	—0·188
1600	0·116	0·014	+0·010
1600	0·336	0·017	—0·036
1600	0·449	0·020	—0·076
1600	0·564	+0·024	—0·126
300	1·192	0	—0·475
410	1·163	0	—0·462
512	1·163	0	—0·467
610	1·175	0	—0·489
700	1·193	0	—0·477

$\theta_{\cdot 7} = -5°$

N	J	C_P	C_T
400	0·464	0·039	—0·106
400	1·346	0·084	—0·610
400	2·400	0·082	—1·130
700	0·265	0·028	—0·041
700	0·770	0·067	—0·254
700	1·285	0·087	—0·572
1000	0·186	0·025	—0·022
1000	0·540	0·043	—0·131
1000	0·840	0·081	—0·307
1300	0·143	0·026	—0·017
1300	0·416	0·034	—0·083
1300	0·645	0·056	—0·190
1600	0·116	0·026	—0·018
1600	0·338	0·030	—0·062
1600	0·415	0·034	—0·084

$\theta_{\cdot 7} = -10°$

N	J	C_P	C_T
400	0·462	0·090	—0·168
400	1·348	0·218	—0·650
400	2·395	0·296	—1·179
700	0·265	0·080	—0·071
700	0·772	0·128	—0·279
700	1·288	0·216	—0·609
1000	0·185	0·079	—0·073
1000	0·541	0·091	—0·167
1000	0·840	0·140	—0·307
1300	0·143	0·078	—0·072
1300	0·416	0·072	—0·134
1300	0·505	0·085	—0·153
1600	0·116	0·078	—0·069

$\theta_{\cdot 7} = -15°$

N	J	C_P	C_T
400	0·464	0·148	—0·188
400	1·346	0·370	—0·689
400	2·400	0·481	—1·172
700	0·265	0·141	—0·117
700	0·770	0·184	—0·291
700	1·285	0·338	—0·640
1000	0·186	0·136	—0·117
1000	0·540	0·154	—0·222
1000	0·840	0·202	—0·331
1300	0·143	0·132	—0·111

$\theta_{\cdot 7} = -20°$

N	J	C_P	C_T
400	0·462	0·226	—0·220
400	1·350	0·509	—0·710
400	2·400	0·711	—1·185
700	0·265	0·206	—0·166
700	0·774	0·274	—0·333
700	1·290	0·485	—0·659
1000	0·185	0·204	—0·148
1000	0·541	0·238	—0·265
1000	0·844	0·284	—0·393
1300	0·143	0·195	—0·147

TABLE 3

Elemental Thrust Coefficients dC_T/dx Obtained from Wake Survey

Blade Design RA25842

N	V	Blade Station $x = r/R$						
		0·45	0·55	0·65	0·75	0·85	0·925	0·975
$\theta_{.7} = 20°$								
1110	59·4	0·171	0·235	+0·304	+0·331	+0·302	−0·041	−0·018
1320	59·4	0·191	0·254	0·341	0·382	0·351	−0·027	−0·009
935	99·5	0·111	0·159	0·180	0·176	0·126	+0·066	−0·004
1110	99·5	0·142	0·203	0·241	0·248	0·205	0·135	−0·013
1320	99·5	0·163	0·238	+0·286	+0·303	+0·268	0·091	−0·014
							+0·019	
935	149·7	0·020	0·012	−0·010	−0·060	−0·129	−0·168	−0·184
1110	149·7	0·076	0·104	+0·103	+0·082	+0·029	−0·024	−0·040
1320	149·7	0·105	0·148	+0·169	+0·161	+0·116	+0·057	+0·004
$\theta_{.7} = 24°$								
935	59·4	0·186	0·242	0·317	0·380	0·382	−0·045	−0·026
							−0·105	
1110	59·4	0·215	0·264	0·350	0·434	0·448	−0·087	−0·018
							−0·157	
1320	59·4	0·224	0·281	0·360	0·451	0·484	−0·110	−0·011
							−0·134	
935	99·5	0·141	0·205	0·253	0·271	0·250	+0·196	−0·017
1110	99·5	0·177	0·258	0·324	0·364	0·347	0·223	−0·022
1320	99·5	0·198	0·281	0·367	0·424	0·420	+0·252	−0·027
935	149·7	0·069	0·097	0·104	0·090	0·049	0	−0·020
1110	149·7	0·123	0·175	0·212	0·220	0·185	+0·127	+0·035
1320	149·7	0·146	0·216	0·267	0·290	0·270	+0·215	0

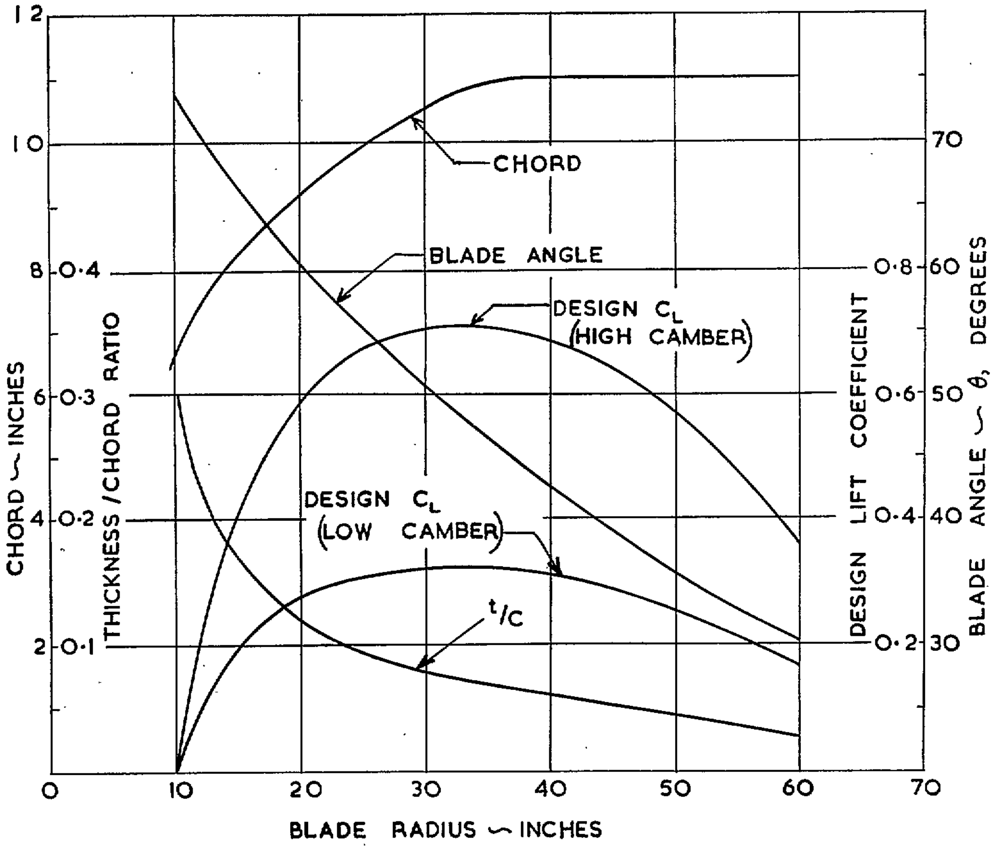

FIG. 1. Blade characteristics.—Blade design: RA25842 (high camber); RA25872 (low camber).

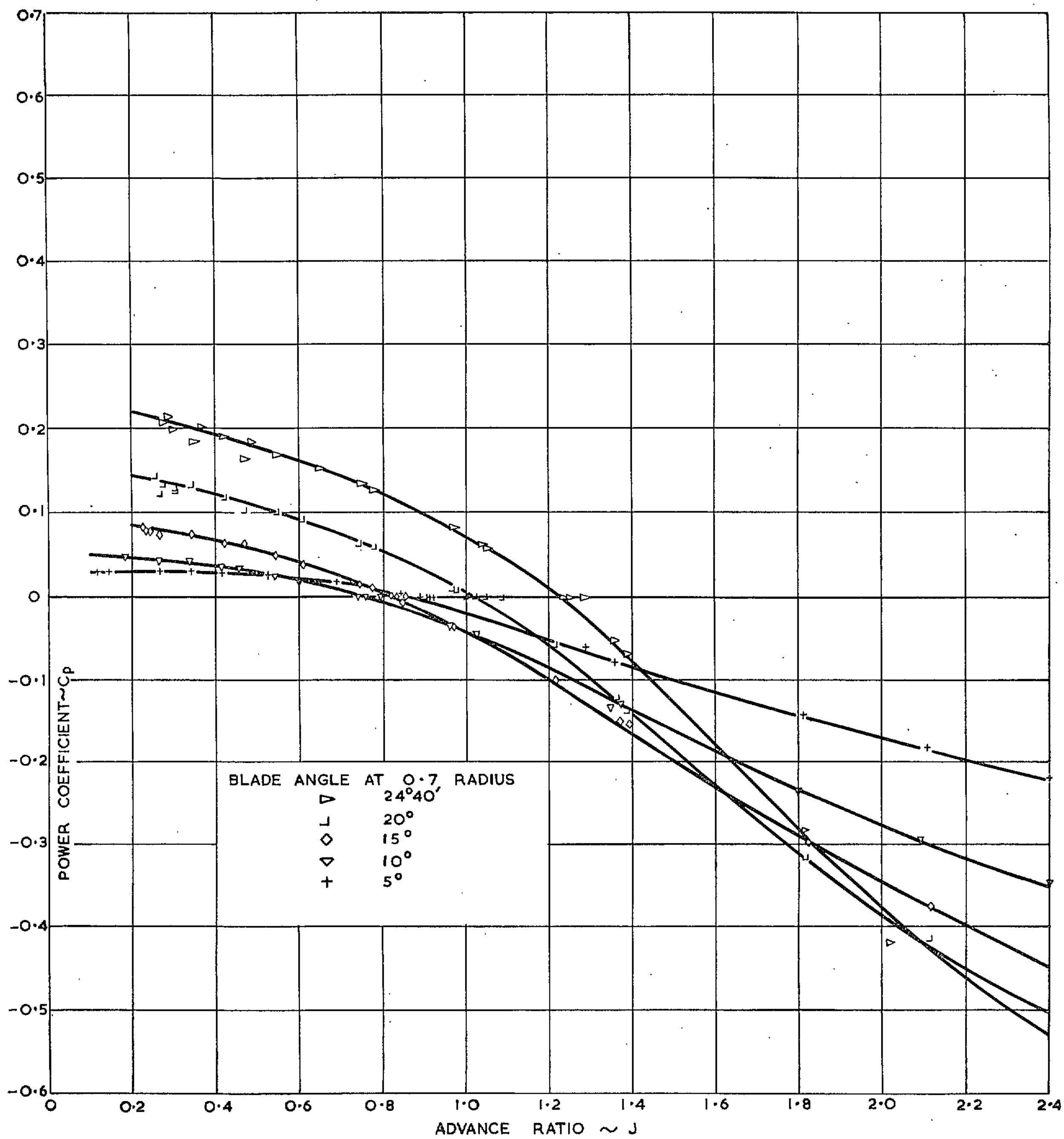

FIG. 2. Power coefficient.—Characteristics of four-bladed propeller with blades RA25842 (high camber). Integrated design lift coefficient: 0·55. Total activity factor: 568.

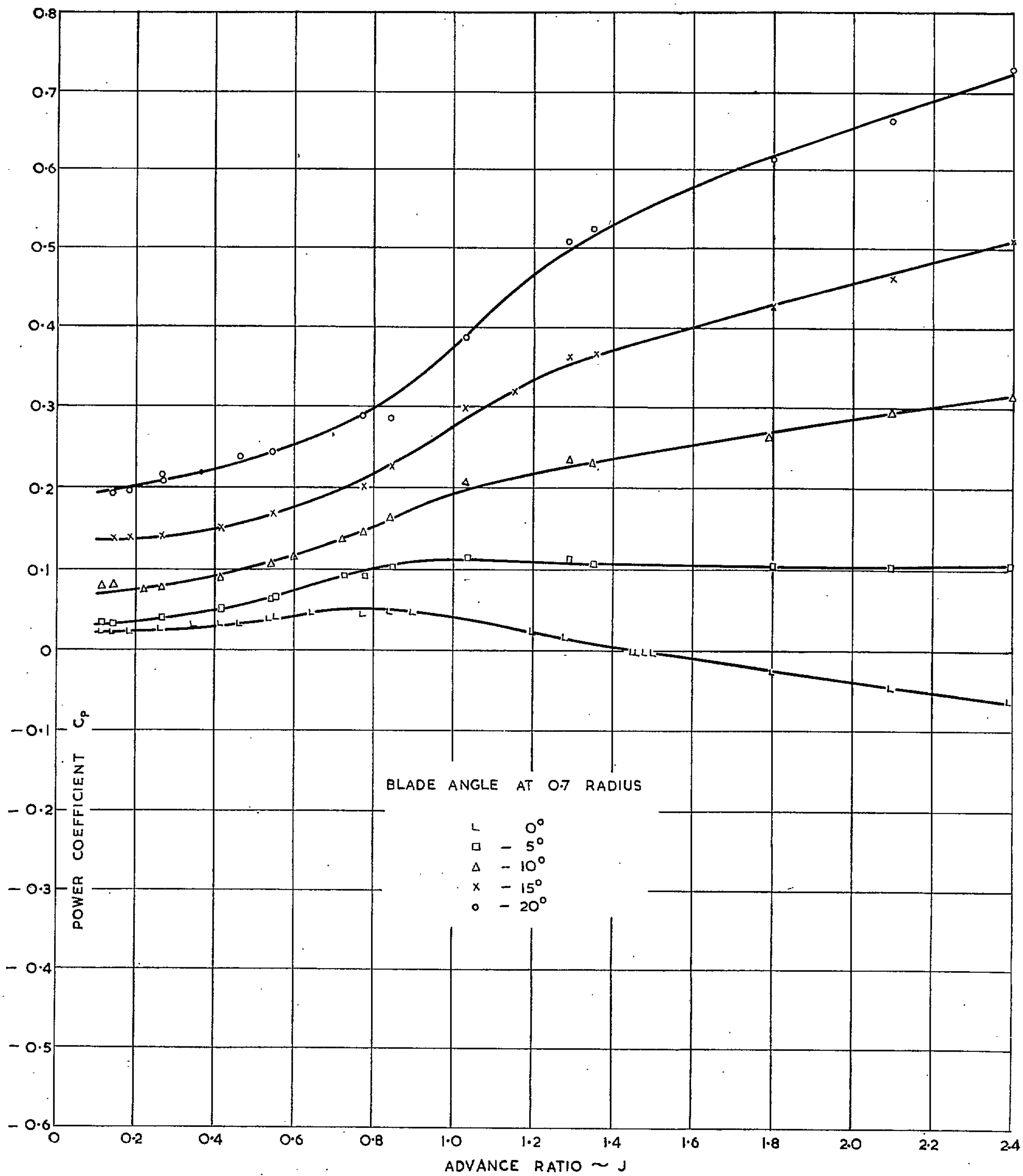

FIG. 3. Power coefficient.—Characteristics of four-bladed propeller with blades RA25842 (high camber). Integrated design lift coefficient: 0·55. Total activity factor: 568.

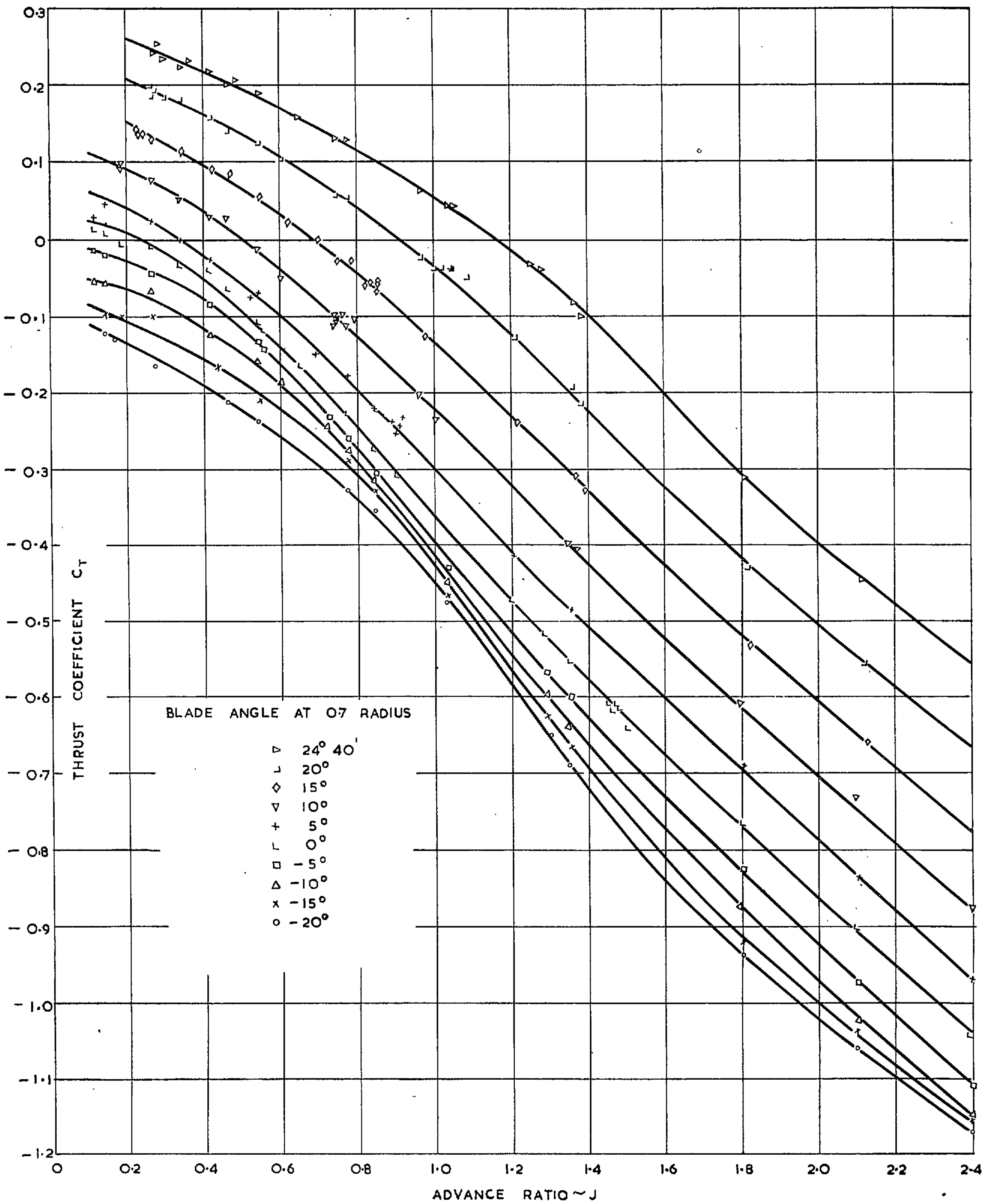

FIG 4. Thrust coefficient.—Characteristics of four-bladed propeller with blades RA25842 (high camber). Integrated design lift coefficient: 0·55. Total activity factor: 568.

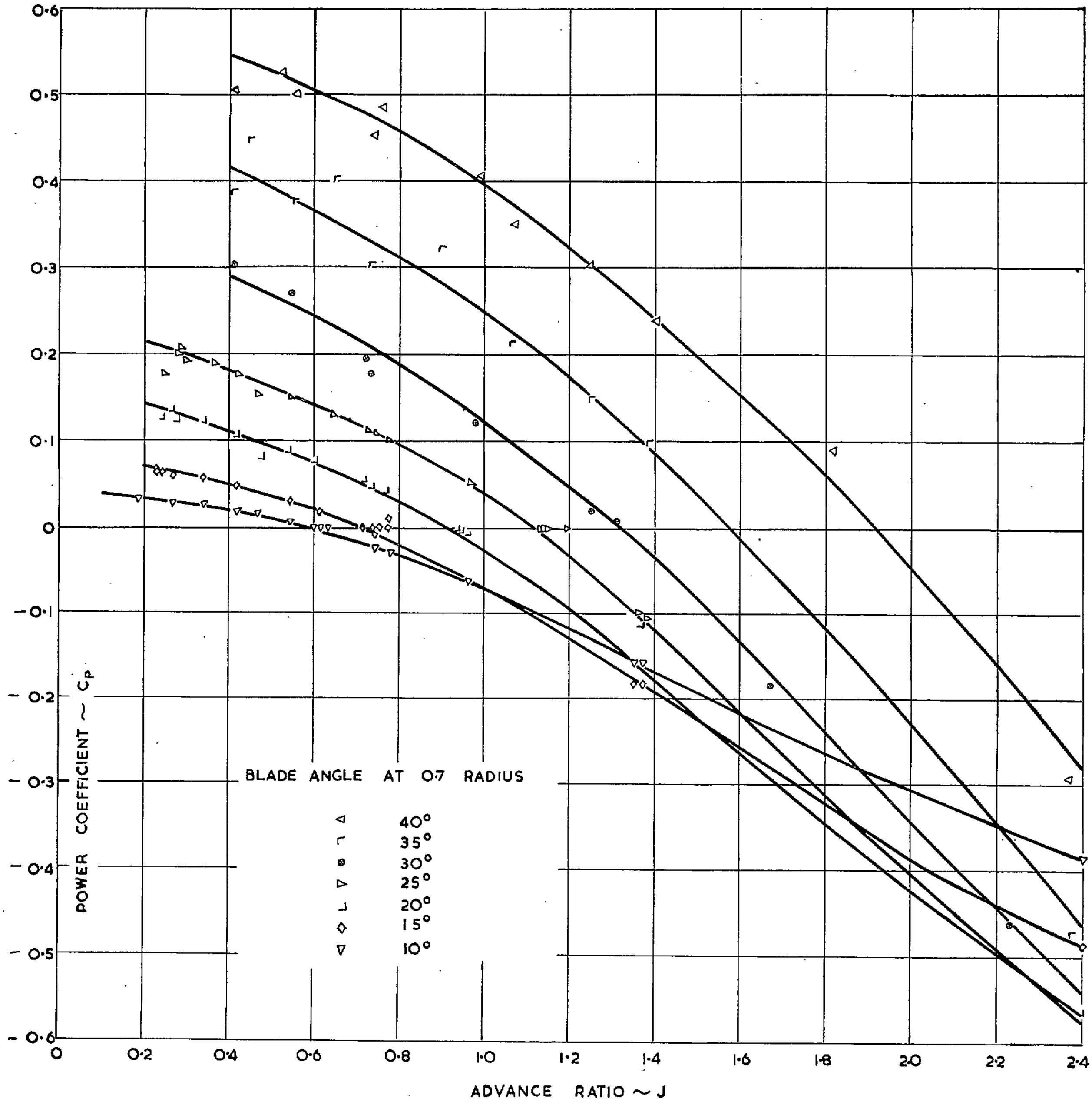

FIG. 5. Power coefficient.—Characteristics of four-bladed propeller with blades RA25872 (low camber). Integrated design lift coefficient: 0·25. Total activity factor: 568.

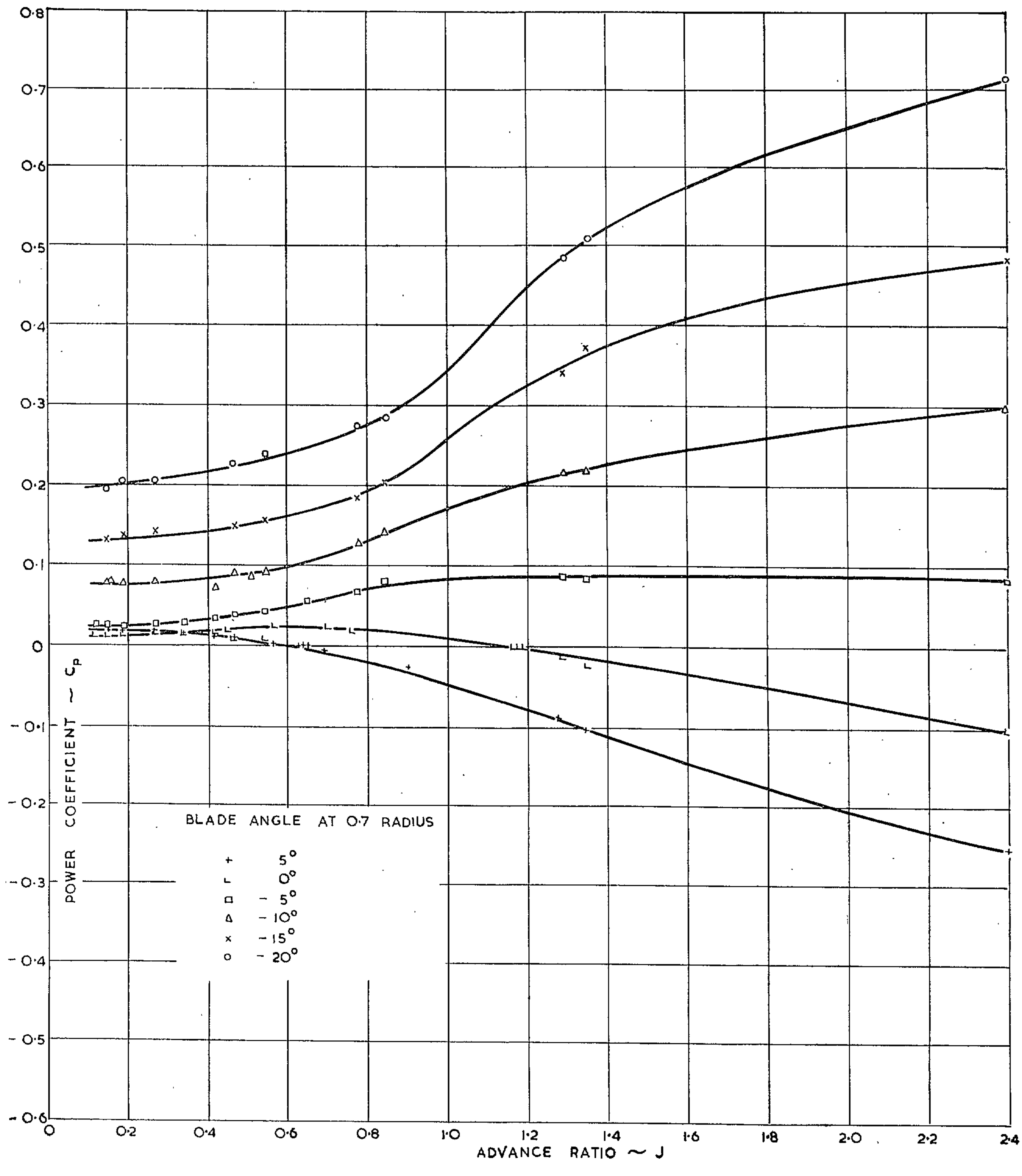

FIG. 6. Power coefficient.—Characteristics of four-bladed propeller with blades RA25872 (low camber). Integrated design lift coefficient: 0·25. Total activity factor: 568.

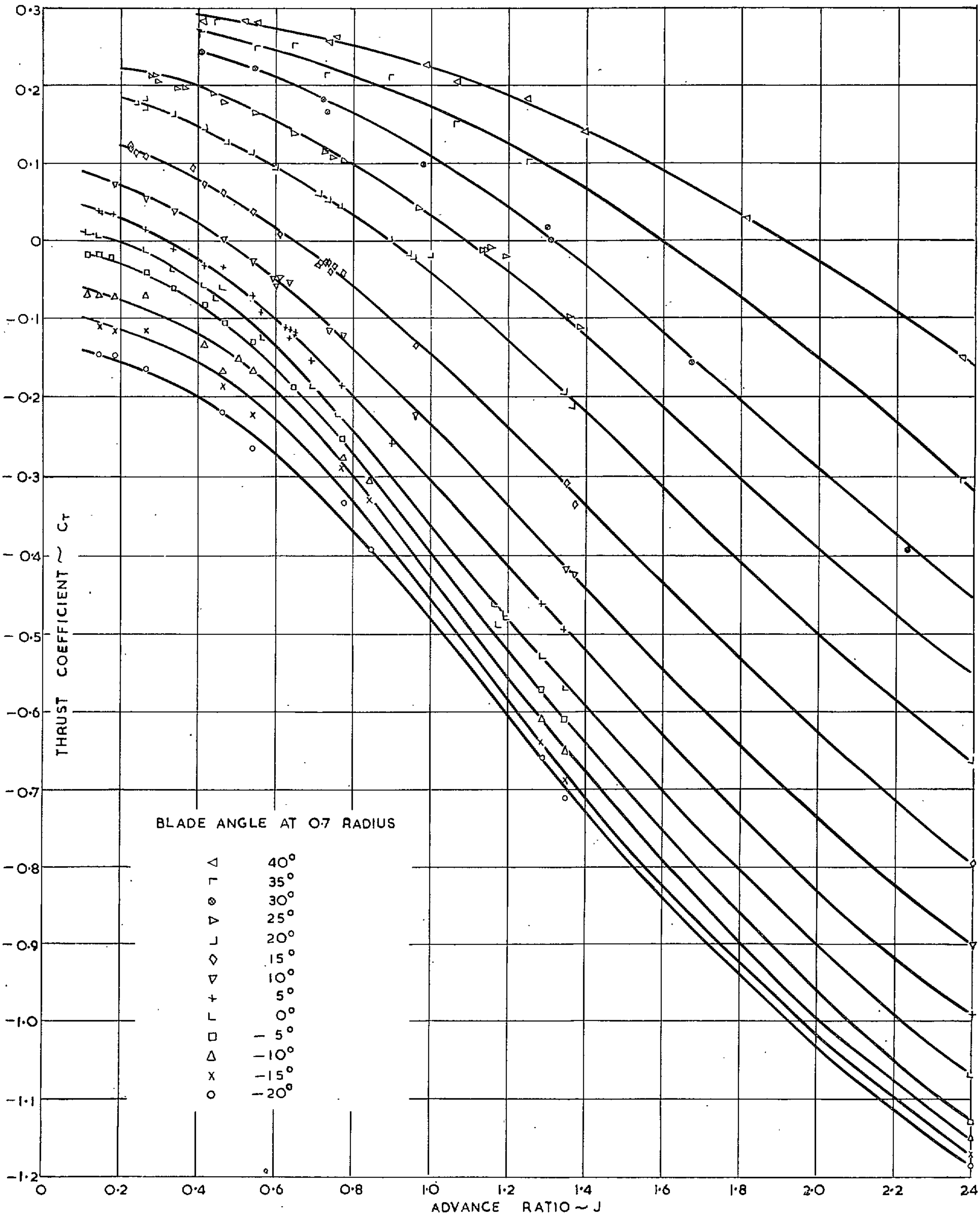

FIG. 7. Thrust coefficient.—Characteristics of four-bladed propeller with blades RA25872 (low camber). Integrated design lift coefficient: 0·25. Total activity factor: 568.

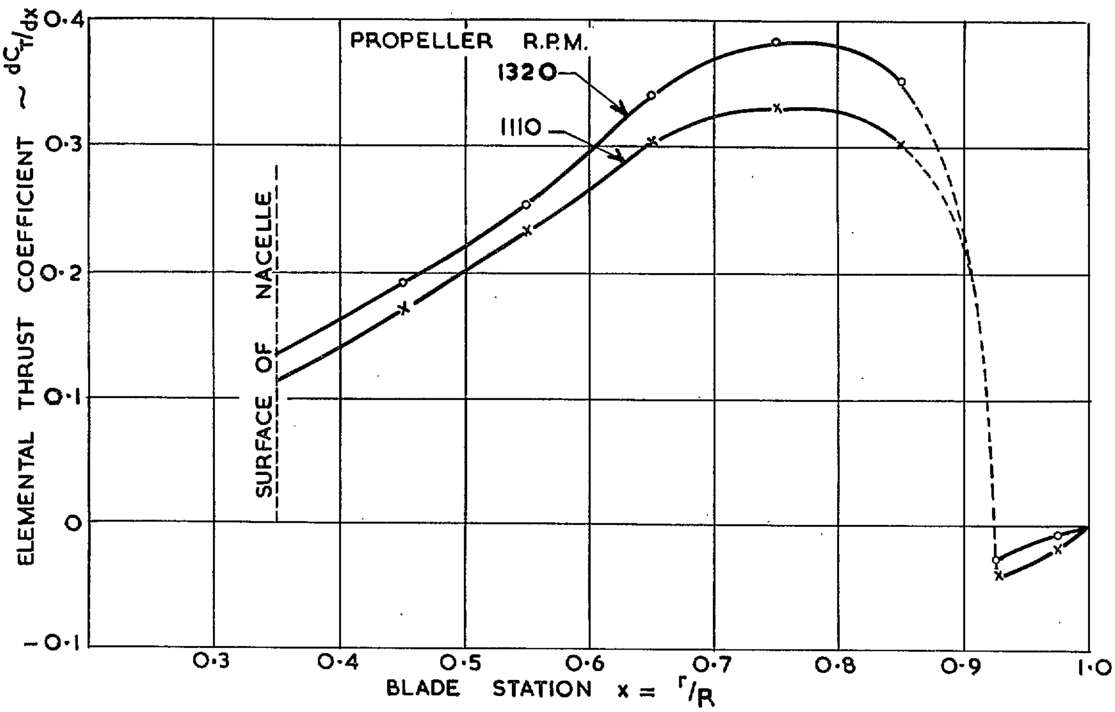

FIG. 8. Blade thrust distribution obtained from wake survey ($\theta_{.7} = 20$ deg; $V = 59 \cdot 6$ ft/sec; Blade design RA 25842).

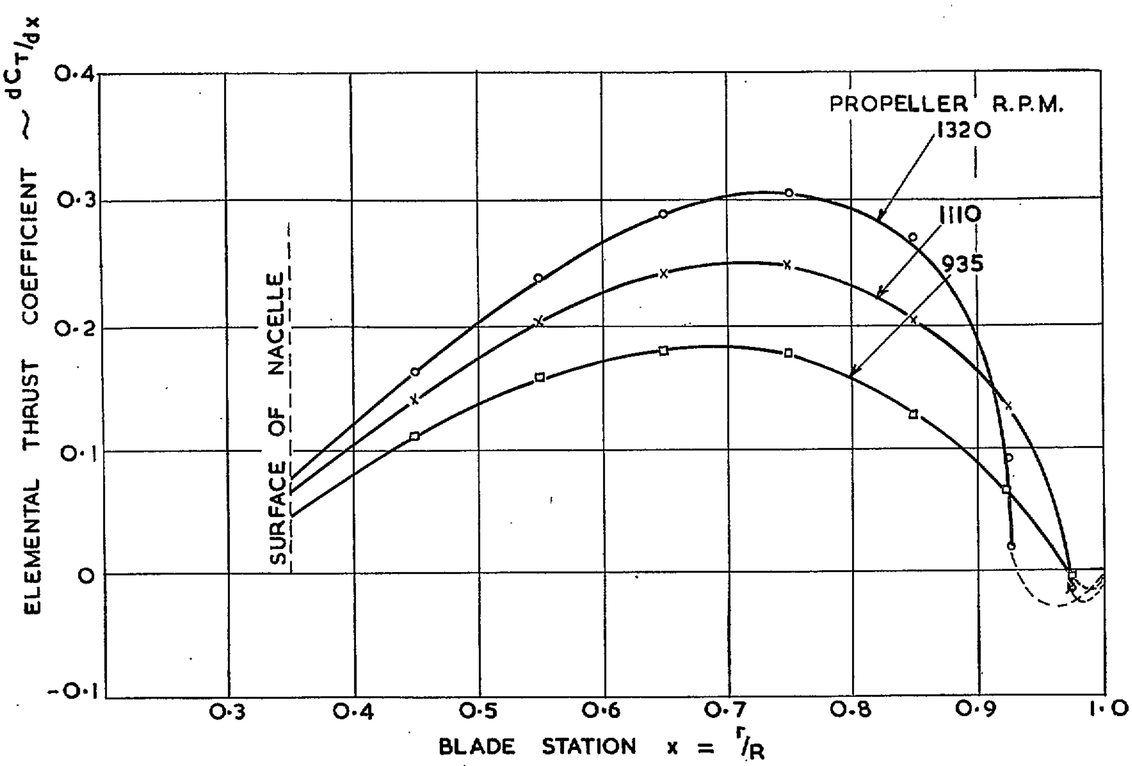

FIG. 9. Blade thrust distribution obtained from wake survey ($\theta_{.7} = 20$ deg; $V = 99 \cdot 5$ ft/sec; blade design RA25842).

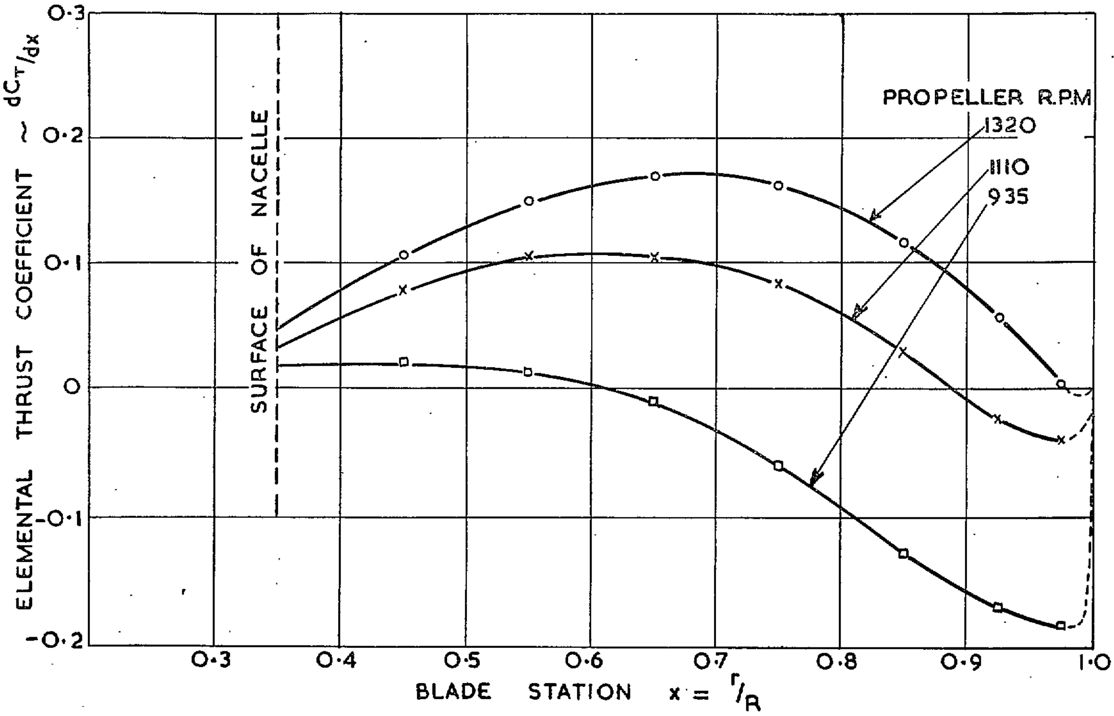

FIG 10. Blade thrust distribution obtained from wake survey ($\theta_{.7}$ = 20 deg; V = 149·7 ft/sec; blade design RA25842).

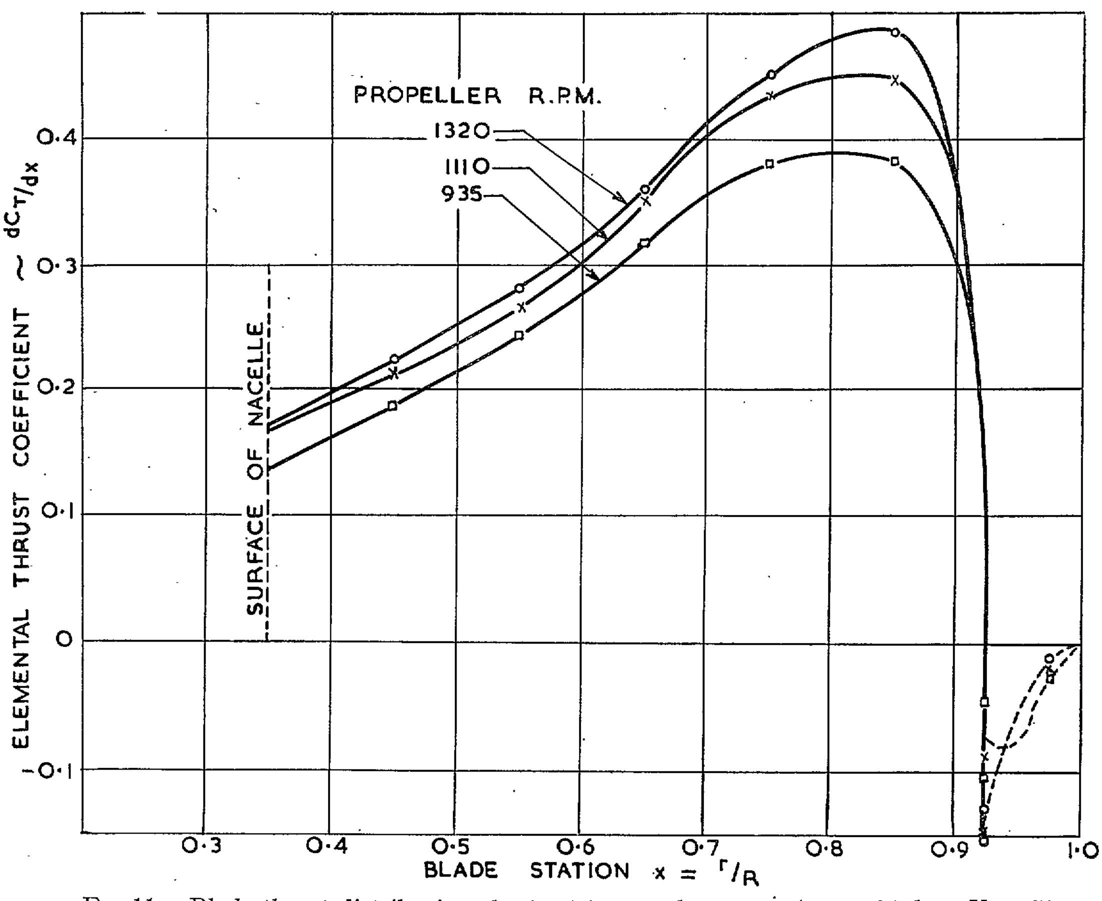

FIG 11. Blade thrust distribution obtained from wake survey ($\theta_{.7}$ = 24 deg; V = 59·4 ft/sec; blade design RA25842).

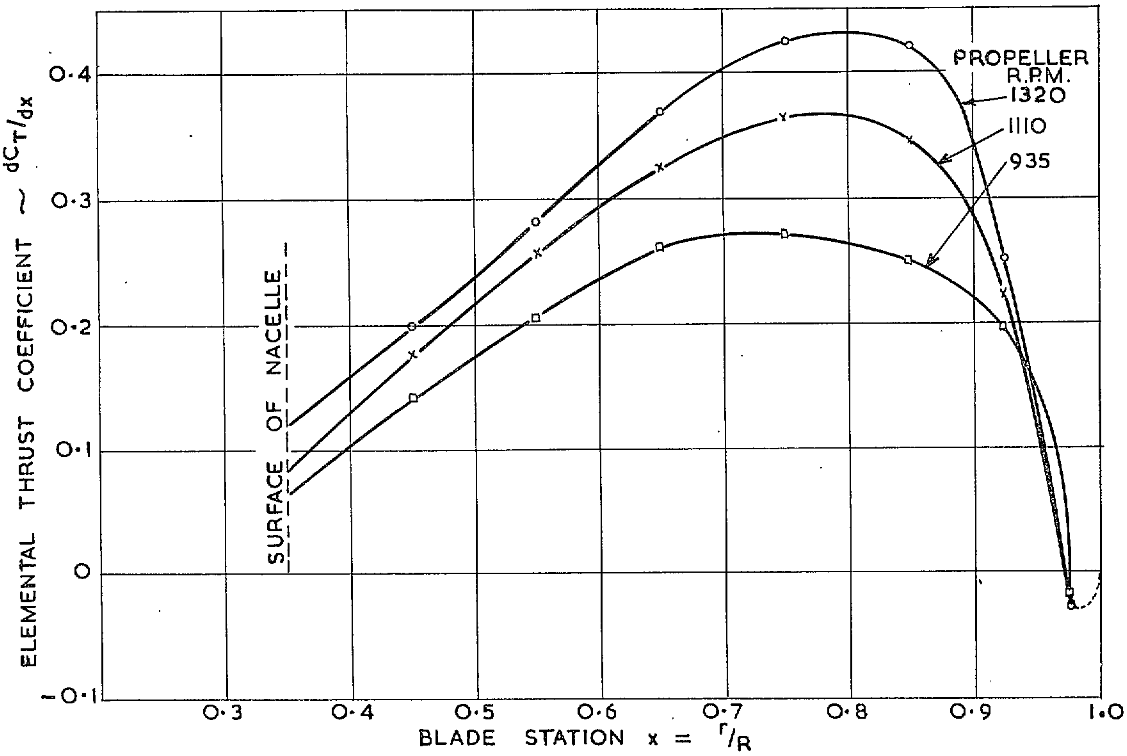

FIG. 12. Blade thrust distribution obtained from wake survey ($\theta_{\cdot 7}$ = 24 deg; V = 99·5 ft/sec; blade design RA25842).

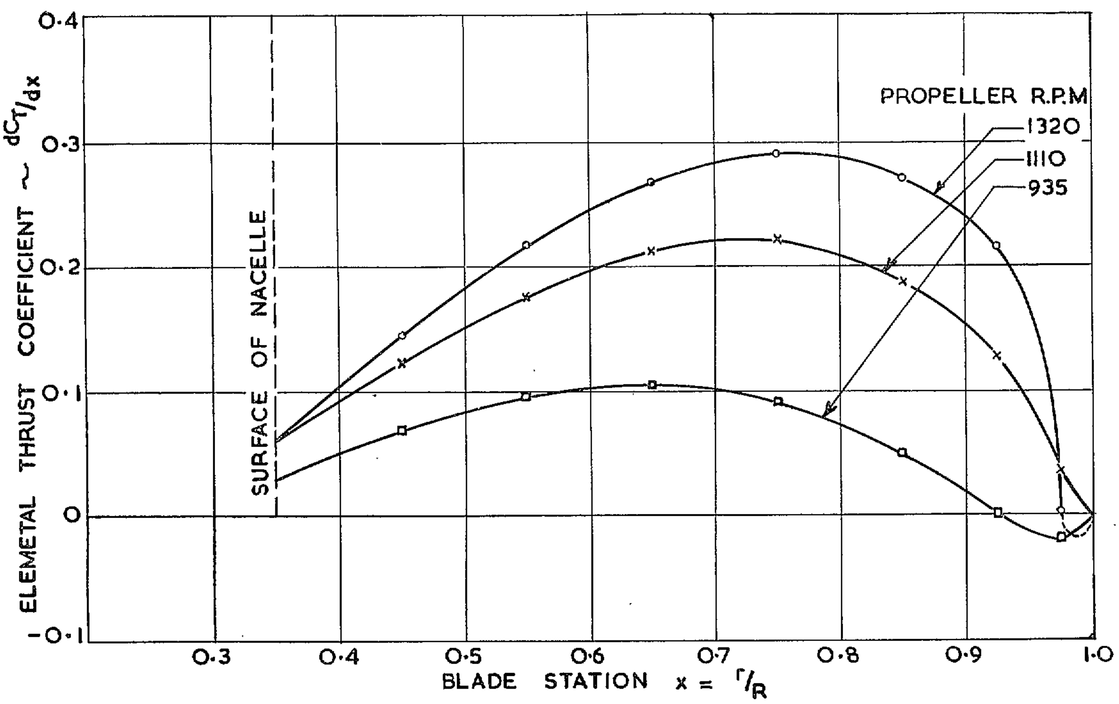

FIG. 13. Blade thrust distribution obtained from wake survey ($\theta_{\cdot 7}$ = 24 deg; V = 149·7 ft/sec; blade design RA25842).

(74080) Wt. 53/2293 K.7 3/59 Hw.

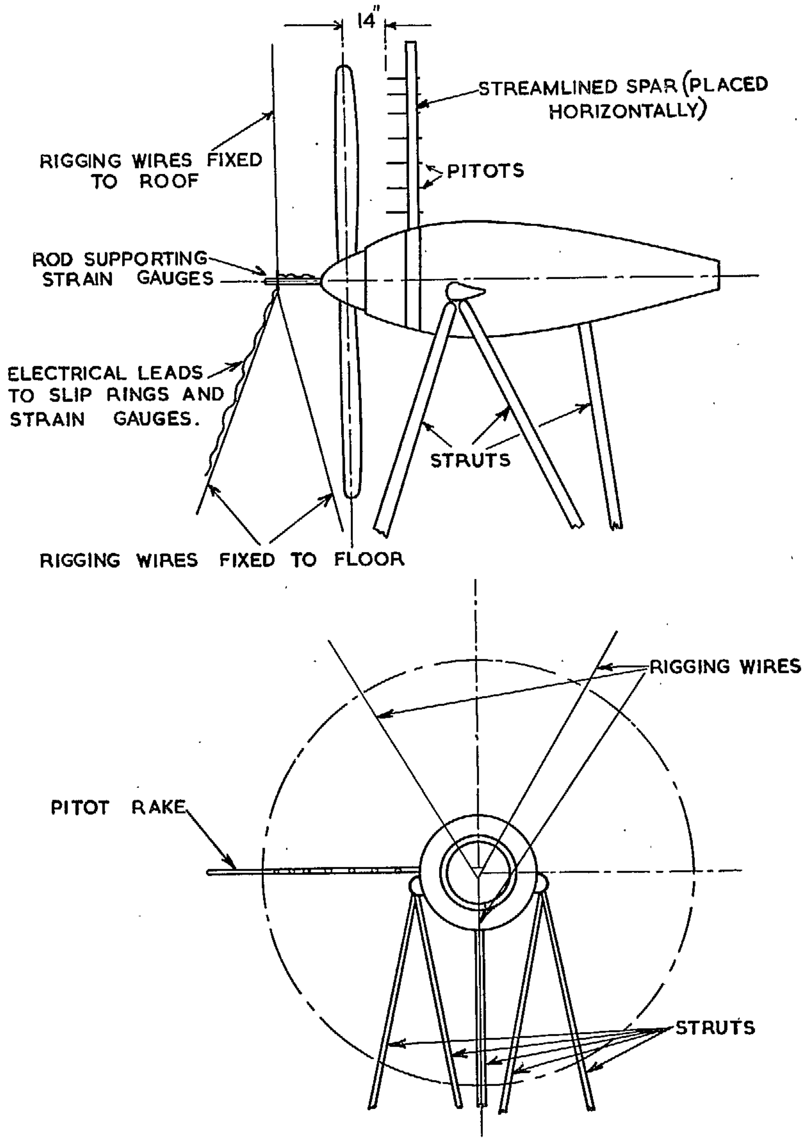

FIG. 14. Diagram showing position of pitots and rigging for strain-gauge equipment.

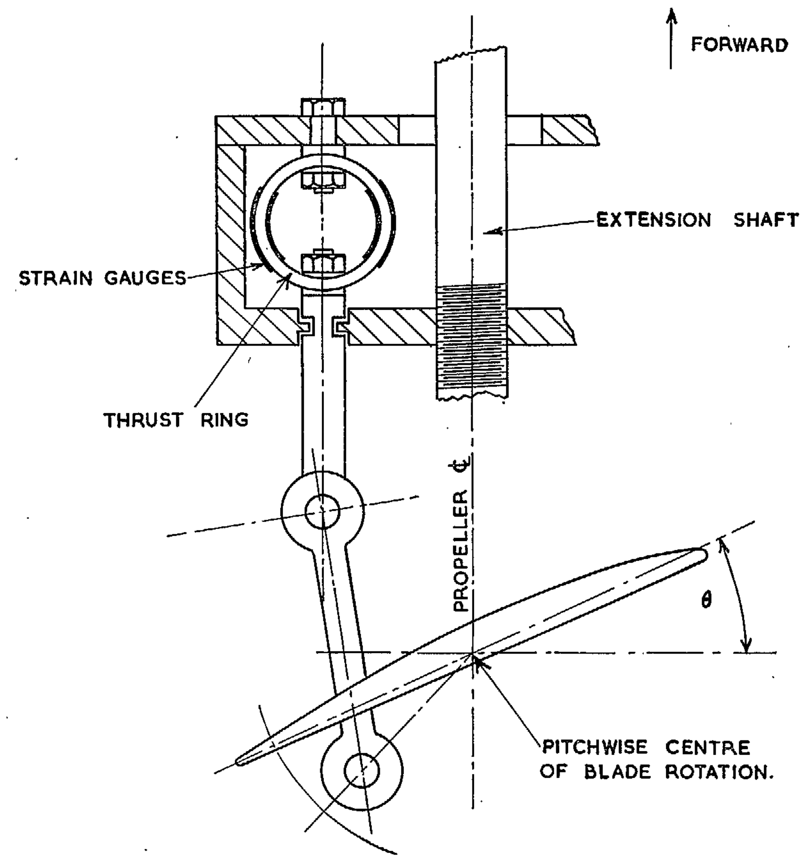

FIG. 15. Propeller link mechanism for measurement of twisting moment.

PRINTED IN GREAT BRITAIN

Publications of the Aeronautical Research Council

ANNUAL TECHNICAL REPORTS OF THE AERONAUTICAL RESEARCH COUNCIL (BOUND VOLUMES)

1939 Vol. I. Aerodynamics General, Performance, Airscrews, Engines. 50*s*. (52*s*.).
Vol. II. Stability and Control, Flutter and Vibration, Instruments, Structures, Seaplanes, etc. 63*s*. (65*s*.)

1940 Aero and Hydrodynamics, Aerofoils, Airscrews, Engines, Flutter, Icing, Stability and Control, Structures, and a miscellaneous section. 50*s*. (52*s*.)

1941 Aero and Hydrodynamics, Aerofoils, Airscrews, Engines, Flutter, Stability and Control, Structures. 63*s*. (65*s*.)

1942 Vol. I. Aero and Hydrodynamics, Aerofoils, Airscrews, Engines. 75*s*. (77*s*.)
Vol. II. Noise, Parachutes, Stability and Control, Structures, Vibration, Wind Tunnels. 47*s*. 6*d*. (49*s*. 6*d*.)

1943 Vol. I. Aerodynamics, Aerofoils, Airscrews. 80*s*. (82*s*.)
Vol. II. Engines, Flutter, Materials, Parachutes, Performance, Stability and Control, Structures. 90*s*. (92*s*. 9*d*.)

1944 Vol. I. Aero and Hydrodynamics, Aerofoils, Aircraft, Airscrews, Controls. 84*s*. (86*s*. 6*d*.)
Vol. II. Flutter and Vibration, Materials, Miscellaneous, Navigation, Parachutes, Performance, Plates and Panels, Stability, Structures, Test Equipment, Wind Tunnels. 84*s*. (86*s*. 6*d*.)

1945 Vol. I. Aero and Hydrodynamics, Aerofoils. 130*s*. (132*s*. 9*d*.)
Vol. II. Aircraft, Airscrews, Controls. 130*s*. (132*s*. 9*d*.)
Vol. III. Flutter and Vibration, Instruments, Miscellaneous, Parachutes, Plates and Panels, Propulsion. 130*s*. (132*s*. 6*d*.)
Vol. IV. Stability, Structures, Wind Tunnels, Wind Tunnel Technique. 130*s*. (132*s*. 6*d*.)

Annual Reports of the Aeronautical Research Council—

1937 2*s*. (2*s*. 2*d*.) 1938 1*s*. 6*d*. (1*s*. 8*d*.) 1939–48 3*s*. (3*s*. 5*d*.)

Index to all Reports and Memoranda published in the Annual Technical Reports, and separately—

April, 1950 - - - - R. & M. 2600 2*s*. 6*d*. (2*s*. 10*d*.)

Author Index to all Reports and Memoranda of the Aeronautical Research Council—

1909—January, 1954 R. & M. No. 2570 15*s*. (15*s*. 8*d*.)

Indexes to the Technical Reports of the Aeronautical Research Council—

December 1, 1936—June 30, 1939	R. & M. No. 1850	1*s*. 3*d*. (1*s*. 5*d*.)
July 1, 1939—June 30, 1945	R. & M. No. 1950	1*s*. (1*s*. 2*d*.)
July 1, 1945—June 30, 1946	R. & M. No. 2050	1*s*. (1*s*. 2*d*.)
July 1, 1946—December 31, 1946	R. & M. No. 2150	1*s*. 3*d*. (1*s*. 5*d*.)
January 1, 1947—June 30, 1947	R. & M. No. 2250	1*s*. 3*d*. (1*s*. 5*d*.)

Published Reports and Memoranda of the Aeronautical Research Council—

Between Nos. 2251–2349	R. & M. No. 2350	1*s*. 9*d*. (1*s*. 11*d*.)
Between Nos. 2351–2449	R. & M. No. 2450	2*s*. (2*s*. 2*d*.)
Between Nos. 2451–2549	R. & M. No. 2550	2*s*. 6*d*. (2*s*. 10*d*.)
Between Nos. 2551–2649	R. & M. No. 2650	2*s*. 6*d*. (2*s*. 10*d*.)
Between Nos. 2651–2749	R. & M. No. 2750	2*s*. 6*d*. (2*s*. 10*d*.)

Prices in brackets include postage

HER MAJESTY'S STATIONERY OFFICE

York House, Kingsway, London W.C.2; 423 Oxford Street, London W.1; 13a Castle Street, Edinburgh 2; 39 King Street, Manchester 2; 2 Edmund Street, Birmingham 3; 109 St. Mary Street, Cardiff; Tower Lane, Bristol 1; 80 Chichester Street, Belfast, *or through any bookseller.*

S.O. Code No. 23-3105

R. & M. No. 310